Am J Transl Res 2015;7(2):385-392
www.ajtr.org /ISSN:1943-8141/AJTR0003241

Original Article

Combined histological and hematological assessment of iron-induced organ damage in a gerbil model of iron overload

Man Wang[1], Rong-Rong Liu[1], Cong-Jun Wang[2], Wei Kang[3], Gao-Hui Yang[1], Wu-Ning Zhong[3], Yong-Rong Lai[1]

[1]Department of Hematology, First Affiliated Hospital of Guangxi Medical University, Nanning, Guangxi 530021, PR China; [2]Department of General Surgery, Third Affiliated Hospital of Guangxi Medical University, Nanning, Guangxi 530021, PR China; [3]Department of Radiology, Tumor Hospital of Guangxi Medical University, Nanning, Guangxi 530021, PR China

Received October 19, 2014; Accepted January 5, 2015; Epub February 15, 2015; Published February 28, 2015

Abstract: Background: Previous studies with gerbil models have suggested that excessive iron exposure causes cardiomyopathy and hepatic injury, but pathological analysis was not comprehensive, preventing a detailed understanding of how the metal induces this damage. Methods and results: Gerbils received single intraperitoneal injections of iron dextran (200 mg/kg) or saline and were then analyzed comprehensively for hematological and histological signs of organ damage. These tests included hematology parameters and determination of liver iron concentration, malondialdehyde levels and glutathione peroxidase activity; examination of heart and liver tissue stained with hematoxylin and eosin, Prussian-blue and Masson stain; and electron microscopy analysis of heart and liver ultrastructure. Iron-overloaded animals showed significantly different hematology parameters and significantly higher liver iron concentrations than saline-injected animals, as well as significantly higher malondialdehyde levels and significantly lower glutathione peroxidase activity. Histology analyses showed cellular damage, iron deposits, and both myocardial and liver fibrosis, while electron microscopy of heart and liver sections showed abundant iron deposition lysosomes, and disordered and swollen mitochondria. All these pathological changes increased with exposure time. Conclusions: This comprehensive assessment of iron overload in a gerbil model suggests that excessive iron deposition induces extensive cellular damage, particularly fibrosis in heart and liver. This damage may be the direct result of iron-mediated lipid peroxide damage and of iron deposition that cause compression of myocardial and liver cells, as well as vascular occlusion.

Keywords: Iron overload, lipid peroxidation, fibrosis, oxidative stress, ultrastructure

Introduction

Iron is a crucial component of hemoglobin with a key role in erythropoiesis, oxygen transportation and storage; in addition, it has important functions in DNA synthesis, respiration and cell metabolism, and it is essential for the function of many cellular enzymes [1-3]. As a transition metal, iron readily undergoes oxidation-reduction reactions between its ferric (Fe^{3+}) and ferrous (Fe^{2+}) states, making it ideal for facilitating numerous biochemical reactions. Too much iron, however, can affect numerous tissues, especially the heart, liver and endocrine glands. Thus, iron overexposure in humans, usually resulting from transfusion-dependent anemia and primary hemochromatosis, manifests clinically as cardiac dysfunction and heart failure, liver dysfunction and cirrhosis, and endocrine abnormalities including hypothyroidism, hypogonadism, and diabetes mellitus [4-8].

How iron overload causes these myriad pathological changes is unclear. This condition causes a similar pathophysiology in the Mongolian gerbil as in humans [9-12], and histological studies in that animal model suggested that iron overload induces hepatic fibrosis and cardiomyopathy [13-15]. However, those studies did not comprehensively examine a wide range of pathological indicators, especially hematological indicators, and they looked at pathology mostly about 10 weeks, leaving unanswered numerous questions about how iron leads to organ damage.

Therefore the present study aimed to perform the most comprehensive analysis to date of tissue damage caused by iron overload and to take the first steps towards exploring the mechanism. A combination of histological and hematological analyses were used, and we examined exposure out to 18 weeks.

Material and methods

Animal model

Female Mongolian gerbils aged 8-10 weeks and free of bacterial pathogens were purchased from the Shanghai Institute of Biological Products (Shanghai, China). The weight of the gerbils ranged from 55 to 75 g. They were housed in a pathogen-free environment in a temperature-and-humidity-controlled room with a 12-h light-dark cycle. They had free access to water and standard rodent diet. Animal facilities conformed to the requirements of the Chinese Ministry of Science and Technology. The study was approved by the Institutional Animal Care and Use Committee of the First Affiliated Hospital of Guangxi Medical University, Nanning, China.

Only gerbils showing fine fur and normal behavior and activity levels were included in our study. Animals were randomly assigned into an iron overload group and a saline group (n = 18 each), with animals in each group randomly assigned into three subgroups (n = 6 each). The three subgroups in the iron overload group received weekly intraperitoneal injections of iron dextran (Sigma-Aldrich, St Louis, USA) at 200 mg/kg. One subgroup received injections for 14 weeks, another for 16 weeks, and the third for 18 weeks. After these periods, all three subgroups were left for 1 week without any injection, followed by a 1-week iron equilibration period. The three saline control subgroups were treated in the same way as the iron overload subgroups, except that the weekly injections contained saline.

The iron overload and saline groups were monitored throughout the study for changes in behavior, weight, and appetite. At the predetermined time points (14, 16, or 18 weeks), one subgroup of iron overload and saline animals were fasted for 12 h, then anesthetized by intraperitoneal injection of sodium pentobarbital (50 mg/kg). Blood, heart and liver were harvested for biochemical and histopathological analysis. Hearts and livers were removed rapidly by mid-sternal thoracotomy and carefully cleared of excess tissue, washed with phosphate-buffered saline (PBS) and weighed.

Hematology analysis and determination of liver iron concentration

Serum was sent to the clinical laboratory of the First Affiliated Hospital of Guangxi Medical University for determination of serum ferritin (SF), cardiac troponin I (cTnI), amino-terminal pro-brain natriuretic peptide (NT-proBNP), aspartate aminotransferase (AST) and alanine aminotransferase (ALT). Liver samples were sent to the Guangxi Center for Analysis and Testing Research for quantitative iron determination by atomic absorption spectroscopy.

Histological characterization and iron deposition in heart and liver

Heart and liver samples were fixed in 10% neutral formalin, paraffin-embedded, sectioned (4 μm), and stained with hematoxylin and eosin (HE) to assess cellular integrity, Prussian-blue to examine iron deposition, or Masson stain to visualize fibrosis. Heart and liver samples were cut into small pieces (approximately 1 mm^3), fixed in 0.1 mmol/L (3%, w/v) sodium cacodylate buffer (pH 7. 4) for 2 h at 4°C, and postfixed in 1% osmium tetroxide. These samples were then embedded in epoxy resin and cut into ultrathin sections (70 nm), stained with uranyl acetate and lead citrate, and observed under a Hitachi H-500 transmission electron microscope.

Malondialdehyde levels and glutathione peroxidase activity in heart and liver

Sections of left ventricular free wall and sections of liver were flash-frozen in liquid nitrogen immediately upon organ removal, and stored at -80°C until analysis. Levels of malondialdehyde were determined using thiobarbituric acid, while glutathione peroxidase activity was measured using the dithio-bis-nitrobenzoic acid method.

Statistical analysis

Statistical analyses were carried out using SPSS 16.0 (IBM, Chicago, USA). Data were expressed as mean ± standard deviation. Differences between the iron overload and saline groups were assessed for significance using the independent-samples t-test. Intra-group

Table 1. Hematology parameters and liver iron concentration in gerbils treated with saline or iron for 14, 16 or 18 weeks

Exposure (weeks)	Group	SF (ng/ml)	LIC (mg/g)	cTnI (ng/ml)	NT-proBNP (pg/ml)	AST (U/L)	ALT (U/L)
14	Saline	15.6±2.1	1.8±0.5	11.9±1.2	331.7±38.8	174.3±7.9	68.8±7.9
	Iron	45.5±6.4[a]	48.3±6.7[a]	22.0±3.6[a]	691.5±69.2[a]	180.0±7.4	77.8±6.3
16	Saline	17.1±3.5	1.7±0.7	12.4±0.8	319.3±38.8	165.8±10.3	67.8±7.2
	Iron	53.5±4.4[a,b]	62.8±7.4[a,b]	25.8±4.1[a,b]	717.7±51.1[a]	238.7±33.0[a,b]	97.0±7.7[a,b]
18	Saline	16.8±2.0	1.6±0.6	13.4±2.0	321.6±54.4	169.2±9.2	68.5±6.1
	Iron	62.2±5.5[a,c,d]	72.6±6.2[a,c,d]	28.2±3.5[a,c]	803.2±37.8[a,c,d]	289.8±15.7[a,c,d]	141.3±8.8[a,c,d]

Footnotes: Data are shown as mean ± SD, n=6 for all subgroups. Abbreviations: SF, serum ferritin; LIC, liver iron concentration; cTnI, cardiac troponin I; NT-proBNP, amino-terminal pro-brain natriuretic peptide; AST, aspartate aminotransferase; ALT, alanine aminotransferase. [a], $P < 0.05$ vs saline; [b], $P < 0.05$ vs 14-week iron; [c], $P < 0.05$ vs 14-week iron; [d], $P < 0.05$ vs 16-week iron.

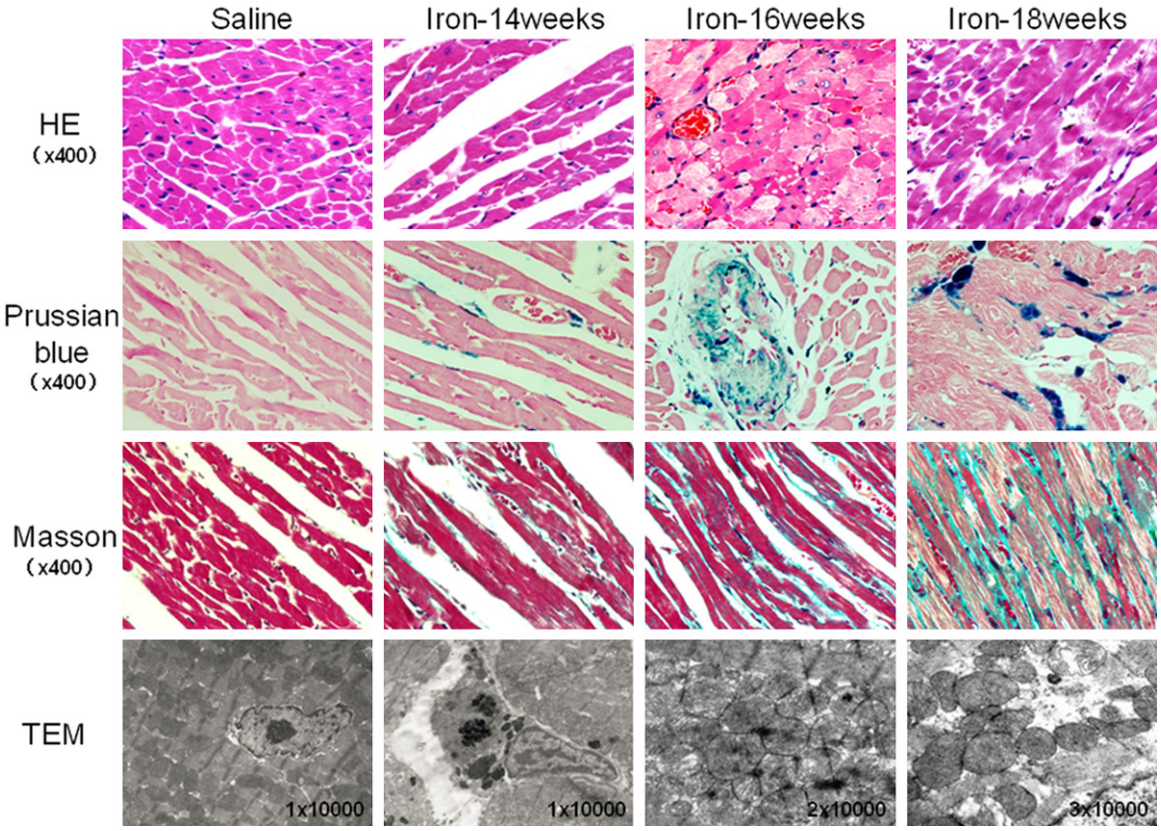

Figure 1. Histology of heart tissue in gerbils treated with saline or iron dextran for 14, 16 or 18 weeks. Tissues were stained with hematoxylin and eosin (HE), Prussian blue or Masson's stain, or they were analyzed by transmission electron microscopy (TEM). HE staining revealed normal cell morphology in the saline group, compared to cell swelling, fatty changes and myocytolysis in the iron overload group. Prussian blue staining revealed no detectable iron deposition in the saline group, compared to numerous iron deposits, mainly around the cell nucleus and blood vessels, in the iron overload group. Masson staining revealed no obvious fibrosis in the saline group, compared to substantial fibrosis in the iron overload group. TEM showed normal cellular architecture in the heart tissue of saline animals, with well-ordered myocardial fibers and no observable electron-dense material. Heart tissue from iron overload animals, however, contained irregularly shaped mitochondria that were often disordered or swollen, as well as electron-dense intracellular deposits (possibly within lysosomes).

differences between 14, 16 and 18 week subgroups were assessed using one-way analysis of variance (ANOVA), followed by a Student-Newman-Keuls test for multiple-comparison

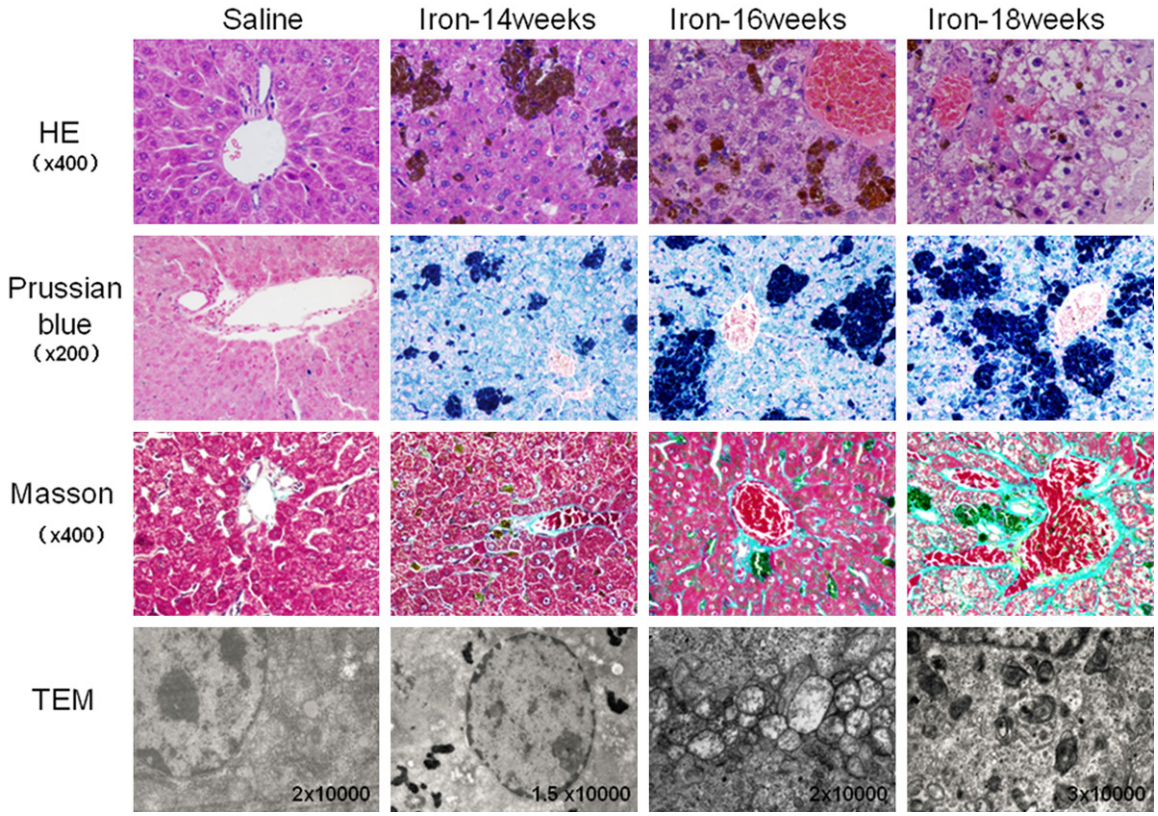

Figure 2. Histology of liver tissue in gerbils treated with saline or iron dextran for 14, 16 or 18 weeks. Tissues were stained as described in **Figure 1**. HE staining showed normal hepatocyte structure and well-ordered hepatic cords in the saline group; iron overload tissue showed hepatocyte swelling, fatty changes, soluble cytoplasm, karyopyknosis and disordered hepatic cords. Prussian-blue staining showed no obvious iron deposition in the saline group, compared to abundant single deposits or deposits in clusters, which were observed primarily in Kupffer cells, hepatocytes and macrophages. Masson staining showed minimal fibrosis in blood vessels in saline animals, compared to obvious, extensive liver fibrosis in iron overload animals. TEM revealed normal organelle structure in saline animals, compared to abundant iron deposits (possibly in lysosomes) around the nucleus, together with mitochondrial swelling and vacuolization.

testing. $P < 0.05$ was considered statistically significant.

Results

Hematology parameters and liver iron concentration

Hematology parameters and liver iron concentration were significantly higher in the iron overload group than in the saline group at 14, 16, and 18 weeks, although AST and ALT levels at 14 weeks were similar between the two groups. None of the hematology parameters or liver iron concentration in the saline group varied significantly over the three time points. Most hematology parameters and liver iron concentration significantly increased over time in the iron overload group, though these increases were not consistent for NT-proBNP or cTnI content. Detailed results are shown in **Table 1**.

Histological characterization and iron deposition in heart and liver

Pathology of heart and liver sections from iron overload animals showed abundant iron deposits associated with cellular swelling, myocytolysis, and nuclear pycnosis; heart tissue showed myocardial cell fatty degeneration, and liver cells showed hepatic steatosis. Myocardial and hepatic tissue also showed necrosis and fiber hyperplasia. Transmission electron microscopy revealed irregularly shaped mitochondria, which often featured disordered, absent cristae and fatty changes. In addition, electron-dense material was observed within myocardial cells and liver cells of iron overload animals, possibly

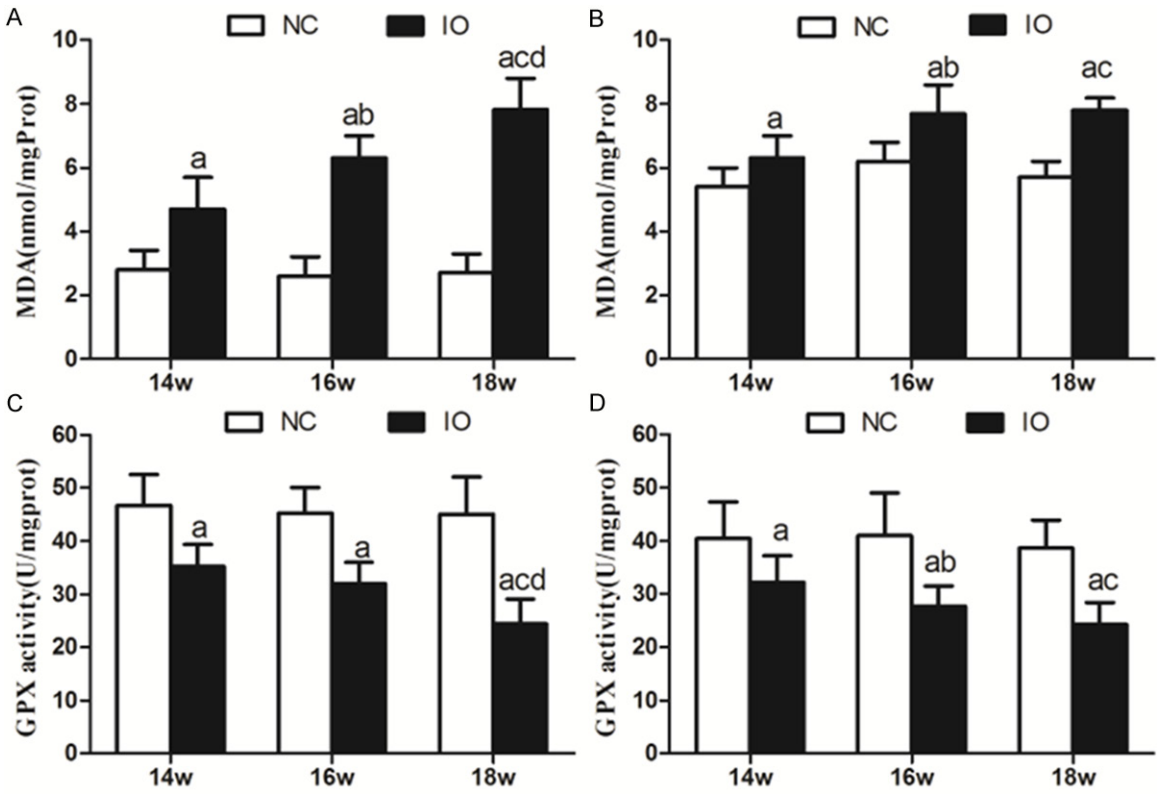

Figure 3. Malondialdehyde (MDA) levels and glutathione peroxidase (GPX) activity in the heart and liver of gerbils treated for 14, 16, or 18 weeks with saline or iron. Malondialdehyde levels (A, B) and glutathione peroxidase activity (C, D) were measured in the (A, C) heart and (B, D) liver. Data are presented as mean ± SD (n = 6 for all subgroups). [a], $P < 0.05$ vs saline; [b], $P < 0.05$ vs 14-week iron; [c], $P < 0.05$ vs 14-week iron; [d], $P < 0.05$ vs 16-week iron.

within lysosomes. All these pathological changes of iron overload animals became worse over time (14-18 weeks), while no significant pathological changes were observed in the saline group even at 18 weeks. The results are shown in **Figures 1** and **2**.

Increased oxidative stress

Iron accumulation inside the heart and liver is expected to lead to oxidative stress caused by free radicals. To verify whether our animal model showed this, we measured malondialdehyde levels, which correlate directly with levels of oxidative stress, and activity of glutathione peroxidase, which correlates inversely with levels of iron-induced oxidative damage. Malondialdehyde levels were significantly higher, and the glutathione peroxidase activity was significantly lower, in iron overload animals than in saline controls at all time points. While these parameters did not vary significantly in the saline group across the three time points, they showed progressive change over time in the iron overload group. Detailed results are shown in **Figure 3A-D**.

Discussion

Here we establish a gerbil model of iron overload and analyze it comprehensively to show that excessive exposure to the metal induces significant histopathology in heart and liver, including cellular degeneration, apoptosis, and fibrosis, all of which worsens with increasing exposure time. Our results suggest that iron overload induces irreversible damage of heart and liver in the absence of effective treatment. Our results directly implicate iron-induced oxidative stress as the cause of many of these changes.

These findings have particular clinical relevance as iron overload becomes more frequent, due to growing numbers of patients who receive iron through prolonged blood transfusion therapy or through intestinal absorption, such as in cases of thalassemia, inherited hemochroma-

tosis, sickle cell anemia and myelodysplastic syndrome [16, 17]. The body cannot effectively excrete excess iron, so prolonged accumulation may lead to problems in the heart, liver and endocrine glands, which can translate clinically into congestive heart failure, hepatic cirrhosis, diabetes, failure of sexual development, osteoporosis, and even early mortality [4-8, 18-20].

In our study, liver iron concentration was significantly higher in iron overload animals than in saline animals at all three time points. This parameter has long been regarded as the gold standard for evaluating body iron content [21], and it can provide more reliable results than measuring serum levels of ferritin, the expression of which is influenced by many factors such as inflammation, infection and chronic disease [22]. In hearts and livers from saline animals, however, staining failed to detect iron. The iron in the overload animals appeared to accumulate in the sarcoplasm, beginning first in the perinuclear areas and spreading to the entire sarcoplasm.

Serum levels of cTnI and NT-proBNP were significantly higher in the iron overload group than in the saline group. Iron overload leads to dysregulation of myocardial L type calcium channels and impairs excitation-contraction coupling, ultimately giving rise to diastolic and systolic dysfunction [23]. Elevated levels of cTnI serve as a highly specific and sensitive marker of myocardial injury, and elevated levels of NT-proBNP indicate asymptomatic left ventricular dysfunction [24, 25].

AST and ALT levels were found to be significantly higher in iron overload animals than in saline controls. This is consistent with the fact that damaged hepatocytes release AST and ALT into the blood. However, our findings contrast with a previous study in a gerbil model of iron overload, which found similar AST and ALT levels between experimental animals and controls after 10 weeks of iron injections [26]. While we also observed similar levels between the two groups after 14 weeks of exposure, we found significantly higher levels in the iron overload group at 16 and 18 weeks. We speculate that 14 weeks may constitute a compensatory phase of liver damage, while 16 and 18 weeks are decompensatory phases.

In our study, both myocardial interstitial fibrosis and liver fibrosis occurred as early as 14 weeks in the iron overload group. This heart and liver fibrosis worsened with increasing exposure time. These results contrast with those of a previous study in a gerbil model of iron overload, which reported fibrous tissue hyperplasia in the liver but not myocardium [27]. Our results are nevertheless consistent with those from a different gerbil model of iron overload, which did show myocardial fibrosis; in this model, the iron chelator deferasirox alleviated cardiac iron overload and subsequently myocardial fibrosis [28]. Together, these results suggest not only that iron overload can significantly affect both the heart and liver, but also that procedures associated with gerbil models may require more standardization and longer exposure periods in order to provide consistent results.

We observed iron-induced structural damage, dysfunction, and disordering (e.g. absence of cristae) in the mitochondria of myocardial cells and liver cells from iron overload animals. We also observed electron-dense material within the cells, possibly within lysosomes. All these pathological changes are consistent with previous studies [29], and with the well-known fact that mitochondria are a direct target of iron damage [30].

Levels of malondialdehye in our iron overload group were significantly higher, and the activity of glutathione peroxidase was significantly lower than in the saline group at all three time points. In fact, this difference increased with increasing exposure time. Iron overload leads to the formation of reactive oxygen species via Fenton and Haber-Weiss reactions, resulting in the peroxidation of membrane lipids, cellular proteins, and nucleic acids [31, 32]. Malondialdehyde, a lipid peroxidation product, serves as an indicator of increased oxidative stress, with higher levels reflecting greater stress. Glutathione peroxidase serves to detoxify peroxides and H_2O_2, so lower levels may be inadequate for protecting cells from oxidative stress. Our results suggest that iron-induced lipid peroxidation produces large amounts of lipid peroxidation products while also reducing the cell's ability to remove free radicals and prevent myocardial injury and liver damage. While our findings are consistent with those of one gerbil model reporting an iron-induced increase in lipid peroxidation and decrease in glutathione peroxidase [33], another gerbil model found that iron overload increased malondialdehyde levels in heart without affecting levels in the

liver [26]. These discrepancies further highlight the potential need to standardize gerbil models of iron overload and make them more rigorous through larger sample sizes and longer follow-up.

Our results provide potentially the most comprehensive analysis to date on effects of iron overload in a gerbil model. They strongly support the idea that iron overload leads to damage and interstitial fiber hyperplasia in multiple organs. This hyperplasia in our model is associated with a significant increase in malondialdehyde levels and significant decrease in glutathione peroxidase activity. It is suggested that iron overload induces interstitial fiber hyperplasia by causing lipid peroxidation damage. We speculate that tissue compression and emphraxis caused by the presence of iron deposits also contribute to iron-induced hyperplasia and other pathological changes. Further studies are needed to explore the mechanism(s) of iron overload toxicity.

Acknowledgements

The work was supported by research grants from Guangxi Natural Science Foundation (grant no. 2011GXNSFD018033), Guangxi Scientific and Technological Research Foundation (grant no. 1140003A-5) and National Natural Science Foundation of China (grant nos. 81260090, 81360085, and 81460025). We thank the technical staff in the Laboratory Animal Centre of Guangxi Medical University and the Department of Pathology and Clinical Laboratory of the Affiliated Hospital of Guangxi Medical University.

Disclosure of conflict of interest

None

Address correspondence to: Yong-Rong Lai, Department of Hematology, First Affiliated Hospital of Guangxi Medical University, No. 6 Shuangyong Road, Nanning, Guangxi 530021, PR China. Tel: +86 771 5352681; Fax: +86 771 5352681; E-mail: laiyongrong_gx@163.com

References

[1] Dunn LL, Suryo Rahmanto Y and Richardson DR. Iron uptake and metabolism in the new millennium. Trends Cell Biol 2007; 17: 93-100.

[2] Andrews PA. Disorders of iron metabolism. N Engl J Med 2000; 342: 1293; author reply 1294.

[3] Hentze MW, Muckenthaler MU and Andrews NC. Balancing acts: molecular control of mammalian iron metabolism. Cell 2004; 117: 285-297.

[4] Jensen CE, Tuck SM, Old J, Morris RW, Yardumian A, De Sanctis V, Hoffbrand AV and Wonke B. Incidence of endocrine complications and clinical disease severity related to genotype analysis and iron overload in patients with beta-thalassaemia. Eur J Haematol 1997; 59: 76-81.

[5] Liu P and Olivieri N. Iron overload cardiomyopathies: new insights into an old disease. Cardiovasc Drugs Ther 1994; 8: 101-110.

[6] Muhlestein JB. Cardiac abnormalities in hemochromatosis. In: Barton JC, Edwards CQ, editors. Hemochromatosis: Genetics, Pathophysiology, Diagnosis, and Treatment. UK: Cambridge University Press; 2000.

[7] Strohmeyer G and Niederau C. Diabetes mellitus and hemochromatosis. In: Barton JC, Edwards CQ, editors. Hemochromatosis: Genetics, Pathophysiology, Diagnosis, and Treatment. UK: Cambridge University Press; 2000.

[8] Abu Rajab M, Guerin L, Lee P and Brown KE. Iron overload secondary to cirrhosis: a mimic of hereditary haemochromatosis? Histopathology 2014; 65: 561-9.

[9] Kaiser L, Davis JM and Schwartz KA. Does the gerbil model mimic human iron overload? J Lab Clin Med 2003; 141: 419-420; author reply 420-412.

[10] Yang T, Dong WQ, Kuryshev YA, Obejero-Paz C, Levy MN, Brittenham GM, Kiatchoosakun S, Kirkpatrick D, Hoit BD and Brown AM. Bimodal cardiac dysfunction in an animal model of iron overload. J Lab Clin Med 2002; 140: 263-271.

[11] Hershko C, Link G, Konijn AM, Huerta M, Rosenmann E and Reinus C. The iron-loaded gerbil model revisited: effects of deferoxamine and deferiprone treatment. J Lab Clin Med 2002; 139: 50-58.

[12] Obejero-Paz CA, Yang T, Dong WQ, Levy MN, Brittenham GM, Kuryshev YA and Brown AM. Deferoxamine promotes survival and prevents electrocardiographic abnormalities in the gerbil model of iron-overload cardiomyopathy. J Lab Clin Med 2003; 141: 121-130.

[13] Al-Rousan RM, Rice KM, Katta A, Laurino J, Walker EM, Wu M, Triest WE and Blough ER. Deferasirox protects against iron-induced hepatic injury in Mongolian gerbil. Transl Res 2011; 157: 368-377.

[14] Wood JC, Otto-Duessel M, Gonzalez I, Aguilar MI, Shimada H, Nick H, Nelson M and Moats R.

Deferasirox and deferiprone remove cardiac iron in the iron-overloaded gerbil. Transl Res 2006; 148: 272-280.
[15] Al-Rousan RM, Paturi S, Laurino JP, Kakarla SK, Gutta AK, Walker EM and Blough ER. Deferasirox removes cardiac iron and attenuates oxidative stress in the iron-overloaded gerbil. Am J Hematol 2009; 84: 565-570.
[16] Burke W, Reyes M and Imperatore G. Hereditary haemochromatosis: a realistic approach to prevention of iron overload disease in the population. Best Pract Res Clin Haematol 2002; 15: 315-328.
[17] Abetz L, Baladi JF, Jones P and Rofail D. The impact of iron overload and its treatment on quality of life: results from a literature review. Health Qual Life Outcomes 2006; 4: 73.
[18] Kim MK, Lee JW, Baek KH, Song KH, Kwon HS, Oh KW, Jang EH, Kang MI and Lee KW. Endocrinopathies in transfusion-associated iron overload. Clin Endocrinol (Oxf) 2013; 78: 271-277.
[19] Rossi F, Perrotta S, Bellini G, Luongo L, Tortora C, Siniscalco D, Francese M, Torella M, Nobili B, Di Marzo V and Maione S. Iron overload causes osteoporosis in Thalassemia Major patients through interaction with TRPV1 channels. Haematologica 2014; 99: 1876-84.
[20] Kew MC. Hepatic iron overload and hepatocellular carcinoma. Liver Cancer 2014; 3: 31-40.
[21] Voskaridou E, Douskou M, Terpos E, Papassotiriou I, Stamoulakatou A, Ourailidis A, Loutradi A and Loukopoulos D. Magnetic resonance imaging in the evaluation of iron overload in patients with beta thalassaemia and sickle cell disease. Br J Haematol 2004; 126: 736-742.
[22] Argyropoulou MI and Astrakas L. MRI evaluation of tissue iron burden in patients with beta-thalassaemia major. Pediatr Radiol 2007; 37: 1191-1200; quiz 1308-1199.
[23] Murphy CJ and Oudit GY. Iron-overload cardiomyopathy: pathophysiology, diagnosis, and treatment. J Card Fail 2010; 16: 888-900.
[24] Fonseca C, Sarmento PM, Minez A, Goncalves E, Covas R, Dias AR, Pina MJ and Ceia F. Comparative value of BNP and NT-proBNP in diagnosis of heart failure. Rev Port Cardiol 2004; 23: 979-991.
[25] Kremastinos DT, Hamodraka E, Parissis J, Tsiapras D, Dima K and Maisel A. Predictive value of B-type natriuretic peptides in detecting latent left ventricular diastolic dysfunction in beta-thalassemia major. Am Heart J 2010; 159: 68-74.
[26] Otto-Duessel M, Aguilar M, Moats R and Wood JC. Antioxidant-mediated effects in a gerbil model of iron overload. Acta Haematol 2007; 118: 193-199.
[27] Kaiser L, Davis JM, Patterson J, Johnson AL, Bohart G, Olivier NB and Schwartz KA. Iron sufficient to cause hepatic fibrosis and ascites does not cause cardiac arrhythmias in the gerbil. Transl Res 2009; 154: 202-213.
[28] Wang Y, Wu M, Al-Rousan R, Liu H, Fannin J, Paturi S, Arvapalli RK, Katta A, Kakarla SK, Rice KM, Triest WE and Blough ER. Iron-induced cardiac damage: role of apoptosis and deferasirox intervention. J Pharmacol Exp Ther 2011; 336: 56-63.
[29] Gao X, Qian M, Campian JL, Marshall J, Zhou Z, Roberts AM, Kang YJ, Prabhu SD, Sun XF and Eaton JW. Mitochondrial dysfunction may explain the cardiomyopathy of chronic iron overload. Free Radic Biol Med 2010; 49: 401-407.
[30] Huang XP, O'Brien PJ and Templeton DM. Mitochondrial involvement in genetically determined transition metal toxicity I. Iron toxicity. Chem Biol Interact 2006; 163: 68-76.
[31] Kremastinos DT and Farmakis D. Iron overload cardiomyopathy in clinical practice. Circulation 2011; 124: 2253-2263.
[32] Philippe MA, Ruddell RG and Ramm GA. Role of iron in hepatic fibrosis: one piece in the puzzle. World J Gastroenterol 2007; 13: 4746-4754.
[33] Zhang Y, Huang Y, Deng X, Xu Y, Gao Z and Li H. Iron overload-induced rat liver injury: Involvement of protein tyrosine nitration and the effect of baicalin. Eur J Pharmacol 2012; 680: 95-101.